

Qualification Meeting

Investigating the Role of miRISC in the Maternal-to-zygotic
Transition in *Drosophila melanogaster*

My name
My date of entry
Department of Molecular Genetics
University of Toronto

Pre-Qualification Meeting Report
Meeting Date and Time:
Location:
Supervisor:
Committee
Exam Committee Member:

Sample Report

Abstract

Animal embryogenesis is initially directed by maternal gene products, while at a later time point, zygotically expressed products take over the control of development. This phase of embryogenesis is referred to as the maternal-to-zygotic transition (MZT). During the MZT, many maternal mRNAs are degraded in two distinct waves: the early wave is orchestrated by maternal products, while the late wave requires zygotic products and thus begins after activation of zygotic transcription (i.e. zygotic genome activation, ZGA). During the *Drosophila* MZT, Smaug (SMG) protein is an essential posttranscriptional regulator that directs the early wave of maternal mRNA clearance, and the timely degradation of SMG protein and mRNA is likely critical for an orderly MZT. Previous lab work has demonstrated the role of RNA-binding proteins Brain tumor (BRAT) and Pumilio (PUM) in smg mRNA decay and implicated their cooperation with miRNA-induced silencing complex (miRISC). My project will further investigate the role of miRISC during *Drosophila* MZT, aiming to evaluate the genome-wide influence of miRISC and elucidate its mechanism of action.

Introduction

Animal embryogenesis is initially directed by maternal mRNAs and proteins loaded into the egg during oogenesis. As development proceeds, the control of embryogenesis is transferred to products of the zygotic genome during a process termed maternal-to-zygotic transition (MZT). During the MZT, many maternal mRNAs are degraded through two temporally distinct phases: the early phase depends only on maternal products, while the late phase requires zygotic products and as such initiates after the zygotic genome activation (ZGA)¹.

In fruit fly *Drosophila melanogaster*, approximately three-quarters of the protein-coding transcriptome is deposited into the embryo, and two-thirds of these transcripts are then cleared during the MZT^{2,3}. One master coordinator of the MZT is Smaug (SMG), a multifunctional RNA-binding protein that is required to destabilize two-thirds of the total degraded maternal mRNAs⁴. Due to SMG's broad influence on global mRNA decay, the timely clearance of SMG protein and smg mRNA is essential for a normal MZT.

The 3' UTR of smg mRNA harbors binding sites for Brain tumor (BRAT), Pumilio (PUM) and microRNAs (miRNAs or miRs), and previous published and unpublished work suggests these binding sites contribute to smg mRNA decay^{4,5}. miRNAs are ~22 nucleotide single-stranded RNA molecules that are capable of inducing transcript decay and translational repression⁶. To achieve this function, miRs form miRNA-induced silencing complexes (miRISCs) with Argonaute proteins (Argonaute 1, or AGO1, in *Drosophila*) and guide miRISCs to targets through miR-mRNA complementarity⁶. Both BRAT and PUM homologs have been shown to interact with AGO1 counterparts in other systems^{7,8}, implicating smg mRNA may be subject to combinatorial regulation by BRAT, PUM and miRISCs during *Drosophila* MZT.

More than 100 maternal and zygotic miRs are present in early *Drosophila* embryos⁹. Such a diverse miR repertoire potentiates the miRISC to destabilize numerous mRNAs, and my project's first aim is to characterize the genome-wide targets of miRISC during the MZT.

Poly(A) tail removal by deadenylase is a common trigger of mRNA destabilization, and studies in multiple systems suggest miRISC induces transcript decay by recruiting the CCR4/NOT deadenylase through a scaffold protein GW182⁶. However, our lab did not detect CCR4/NOT as an interactor of GW182 in *Drosophila* embryos by immunoprecipitation-mass spectrometry (IP-MS), nor in IP/westerns. Thus, my second aim is to elucidate the mechanism of miRISC-mediated mRNA decay.

Aims

1. Identify the genome-wide targets of miRISC during the MZT.
2. Elucidate the mechanism of miRISC-mediated mRNA decay during the MZT.

Experimental Plans and Progresses

Aim 1: Identify the genome-wide targets of miRISC during the MZT.

The lab hypothesized that smg mRNA is subject to combinatorial regulation by BRAT, PUM, and miRISCs based on three pieces of evidence: the 3' UTR of smg harbors binding sites for all three regulators; disruption of each regulator leads to partial smg mRNA stabilization; and homologs of BRAT, PUM, and AGO1 have been shown to interact in other systems^{7,8}. Since previous lab members have generated target lists for BRAT and PUM in early embryos, a list of miRISC targets is the last piece of missing information to assess the extent of their cooperation. In addition, a genome-wide analysis of miRISC targets in the early embryo would also be informative on its own to the understanding miRISCs' role during the fly MZT. To achieve this

goal, our lab has proposed to identify miRISC-bound transcripts biochemically by RNA immunoprecipitation-sequencing (RIP-seq), and also to genetically identify miRISC-regulated targets as stabilized mRNAs in embryos depleted of AGO1.

Aim 1a: biochemically identify miRISC-bound transcripts during the MZT.

For the biochemical approach, xxxx performed RIP using 0-2hr and 2-4hr embryos with anti-AGO1 antibody or control irrelevant IgG, and three replicates of each condition together with input total RNA were sent for sequencing. By the last meeting, I had processed the sequencing data following my pipeline (Fig 1A) and identified xxxx out of xxxx genes as targets in 0-2hr samples, and xxxx out of xxxx in 2-4hr samples (Fig 1B). The increase in target number at the later time point is consistent with the higher AGO1 expression level and a more diverse miR repertoire after the zygotic genome activation. As the targets were identified from two consecutive time windows, an expected overlap is observed between the two target lists (Fig 1C).

After identifying miRISC targets from RIP-seq, I then validated the results by confirming three expected characteristics. According to the established model, miRISCs recognize their targets by miRNA-mRNA complementarity and silence expression by inducing mRNA decay/translational repression. Therefore, I expect miRISC targets to contain miRNA binding sites, be enriched for unstable transcripts, and be enriched for translationally repressed transcripts. Because binding of miRNA seed region (nucleotide 2-7) is necessary for target recognition and often happens in the 3' UTR of target transcripts, I mapped the seed matches for all expressed miRNA on the 3' UTR for the most abundant isoforms of each expressed genes (those with TPM > 1 in all 3 replicates of total RNA-seq)⁹. As expected, AGO1 targets contain more miRNA seed matches in their 3' UTR than non-targets in both time points (Fig 2A). To further validate this result, I also performed the same analysis using the more conserved miRNA-target mRNA predications in the TargetScan database¹⁵ and detected the same trend (Fig 2B). Another factor affecting miRNA binding is the local accessibility of the miR binding site within the target mRNA, such that sites that are not participating in extensive intra-mRNA base pairing are more likely to be functional. Therefore, I computationally assessed the accessibility of all miRNA seed matches as we have done previously¹⁶ and assigned each site a score between 0 to 1, with 1 suggesting the site is always accessible. Then I calculated the average of each miRNA's best score for each 3' UTR, and as expected, miRNA matches are more accessible on AGO1 targets than non-targets (Fig 2C).

To determine if AGO1 targets are enriched for unstable transcripts, I compared my AGO1 targets to an unpublished lab dataset, where transcripts expressed during 0-5hr of embryogenesis are grouped into xxxx clusters based on their expression profiles. AGO1 targets are enriched in 4 clusters, all of which are degraded at some point over the first 5 hours of embryogenesis (Fig 2D). At both time points, about xxxx% of AGO1 targets belong to cluster 7/8, and they cover xxxx% of detected genes in these two clusters. To assess the translational status of AGO1 targets, I made use of an external dataset where translation efficiency was assessed by ribosome footprinting¹⁸, and AGO1 targets are enriched in translationally repressed mRNAs (Fig 2E).

To identify the potential roles of miRISC during the MZT, I performed a GO term enrichment analysis for both target lists with gProfiler2¹⁷, using the input RNA from the AGO1 RIP-seq experiments as background. The 0-2hr list is significantly enriched for xxxx GO terms, and the 2-4hr list has xxxx terms. As a high odds ratio (OR) indicates a stronger enrichment, I ordered these terms by decreasing OR and identified three interesting and interconnected themes.

The first is cytoskeletal dynamics (Fig 3A), whose GO terms not only have high ORs and also contain some of the most confident AGO1 target mRNAs. When I ordered AGO1 targets by their fold enrichment in AGO1 RIPs versus input RNA, approximately half of the top 20 hits are cytoskeleton-related (blue cells in Fig 3B). Given early embryos are undergoing rapid nuclear divisions, regulation of cytoskeletal dynamics by AGO1 could be biologically relevant. Similarly, the process of cellularization is also characterized by complex cytoskeletal rearrangements that AGO1 could regulate. The second theme is signaling (Fig 3C). The top term in this category, Rab signaling, participates in cytoskeleton regulation, while others help control cell fate commitment and cell division. The third theme is transcription factor (Fig 3D). Some of the TFs are downstream of signaling pathways, some regulate body pattern determination, and an important one is *zelda*, a so-called pioneer transcription factor that is required for zygotic genome activation.

Future directions: I plan to first follow up on the potential role of miRISC in regulating cytoskeletal dynamics. As a preliminary experiment, I will collect early embryos subject to zygotic and/or maternal AGO1 RNAi knockdown and perform fluorescence staining. DAPI staining may reveal impaired nuclear division, phalloidin staining will allow visualization of actin filaments, and anti-peanut staining will decorate microtubules and reveal potential defects in cytokinesis.

Another interesting target to follow up is GW182, a protein that AGO1 recruits to induce gene silencing. I hypothesize AGO1 may regulate its own activity by targeting GW182, and I will assess this initially by determining GW182 protein level in AGO1 KD embryos.

Aim 1b: genetically identify miRISC-regulated transcripts during the MZT.

The second approach is to identify miRISC targets genetically in early embryos, namely transcripts that are stabilized in an AGO1 loss-of-function background. Because AGO1 mutants are lethal, our lab has constructed an AGO1 transgene that carries a blue-light-inducible degron to achieve a conditional loss of AGO1¹⁹. The light-oxygen-voltage-sensing (LOV) domain unfolds upon blue light irradiation, exposing an N-terminal arginine residue that targets the protein for rapid degradation. A ubiquitin moiety is fused to the extreme N terminus of the LOV domain. Upon translation of this construct, Ub is cleaved off the protein to generate the N-terminal Arg residue. An HA epitope is integrated to allow convenient detection of the transgenic AGO1 protein (See Fig 4A for construct design).

Six fly lines have been generated with the transgene randomly inserted onto the third chromosome, and by the last meeting I've confirmed protein degradation upon prolonged blue light exposure (Fig 4B). I then set out to determine whether this transgene can rescue the loss of endogenous AGO1 and to optimize the conditions to achieve efficient protein degradation.

To determine whether the transgene rescues the loss of AGO1, I used AGO1^{k00208}, an AGO1 allele where the gene is disrupted by a P-element insertion, and attempted to construct rescue fly lines following the cross scheme in Fig 4C. I obtained adult AGO1^{-/-} flies and have confirmed the loss of endogenous AGO1 by Western blot using female ovaries, where AGO1 is highly expressed (Fig 4D). Unfortunately, the transgene rescues only female fecundity but not male fertility. This may result from a background mutation on the AGO1^{k00208} chromosome, and I am currently trying another allele with an early stop codon AGO1^{Q127X} (Fig 4E). If fertility issue arises from low AGO1 level in the male germline, an alternative approach is to mate rescue virgins to w¹¹¹⁸ males because the majority of AGO1 protein in early embryos is translated from maternal AGO1 mRNA.

The goal of optimization was to achieve protein clearance in a shorter time without causing phototoxicity, and I used a line that rescues for optimization. As shown in Fig 4B, blue light exposure for 3h at an intensity of 1200 Lux largely depleted the transgenic AGO1, thus I expected a higher intensity would require shorter exposure time. I first confirmed that 4-hr exposure to 10,000 Lux and 5,000 Lux is not lethal for 4-5 w¹¹⁸ embryos (Fig 4F). I then determined AGO1 protein levels in 3-4hr embryos exposed to 10,000 Lux or 5,000 Lux for 2h or 1h, and surprisingly, a lower intensity seems to achieve better clearance (Fig 4G).

Future directions: If I succeed in establishing a stock of AGO1 rescue flies and achieving efficient AGO1 clearance, I will then use this loss-of-AGO1 model to assess whether individual putative AGO1-bound transcripts are upregulated and whether AGO1-regulated biological processes are disrupted. If this attempt fails, I will use the well-established RNAi knockdown to serve as my loss-of-AGO1 model and continue with the proposed experiments.

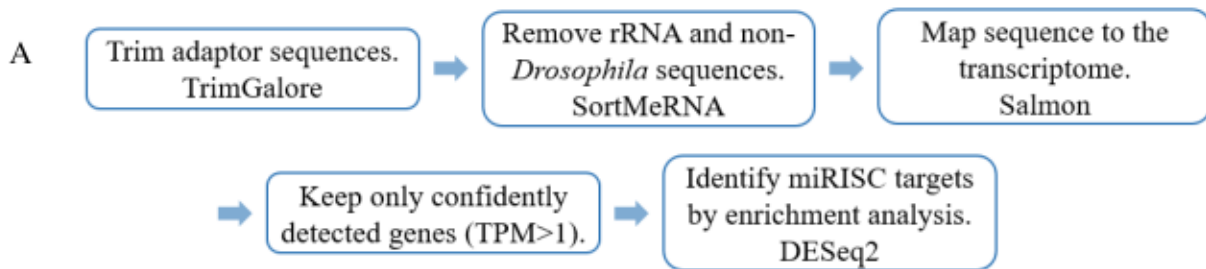
Aim 2: Determine the mechanism of miRISC-mediated mRNA decay during MZT.

Poly(A) tail removal by deadenylases is a common trigger of mRNA destabilization, and work in multiple systems suggests miRISCs induce transcript decay by recruiting the CCR4/NOT deadenylase through a scaffold protein GW182⁶. While we detect a strong interaction between AGO1 and GW182 during the MZT, we failed to detect CCR4/NOT as a potent interactor of GW182 in *Drosophila* embryos by IP-MS or by IP-Western. Thus, miRISC may employ a potentially novel mechanism to achieve gene silencing in early embryos.

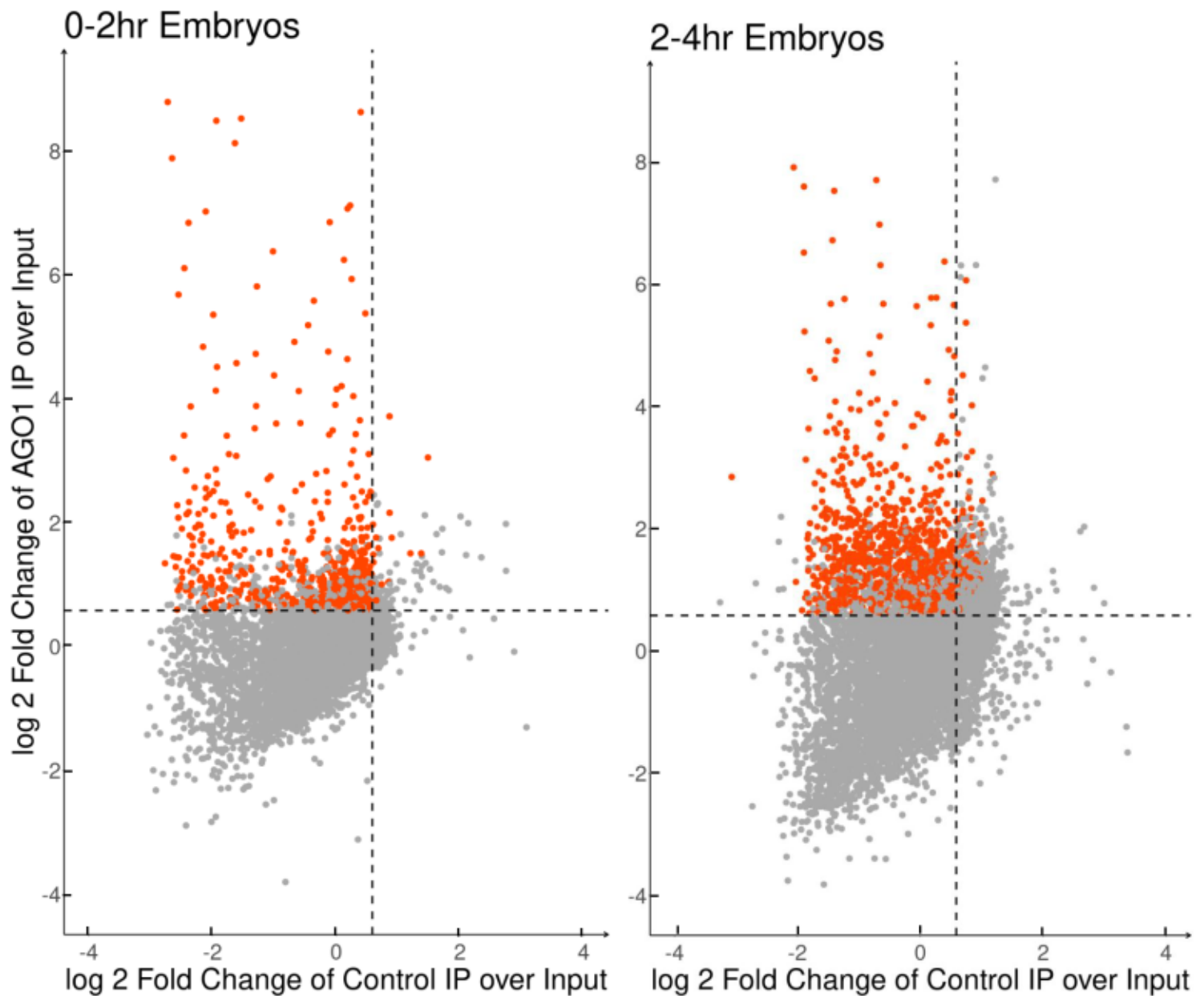
Since AGO1 is required for embryogenesis and GW182 shows strong interaction with AGO1, I first used hatch rate to determine if GW182 is required for embryogenesis. Interestingly, zygotic knockdown of GW182 did not result in any hatch rate defect, while maternal knockdown is embryonic lethal (Fig 5A).

My next step would be to examine whether AGO1 targets are degraded in a GW182-dependent manner. I will knock down GW182 expression via RNAi both zygotically and maternally, and then assess transcript kinetics by RT-qPCR for 10 AGO1 targets and 3 non-targets identified in aim 1a. I expect to observe stabilization of AGO1 targets upon GW182 knockdown but not for non-targets. An alternative approach would be to use a reporter construct harboring miR-binding sites on its 3' UTR, and disruption of the miR pathway is expected to result in reporter upregulation. Such reporters have been constructed and the construction of transgenic lines is in progress.

If GW182 is required for miRISC function, I will use RNAi to assess a list of GW182 interactors that were previously identified by IP-MS. If not, I will perform IP-MS against AGO1 in early embryos and then screen AGO1 interactors as described above for GW182.



B



C

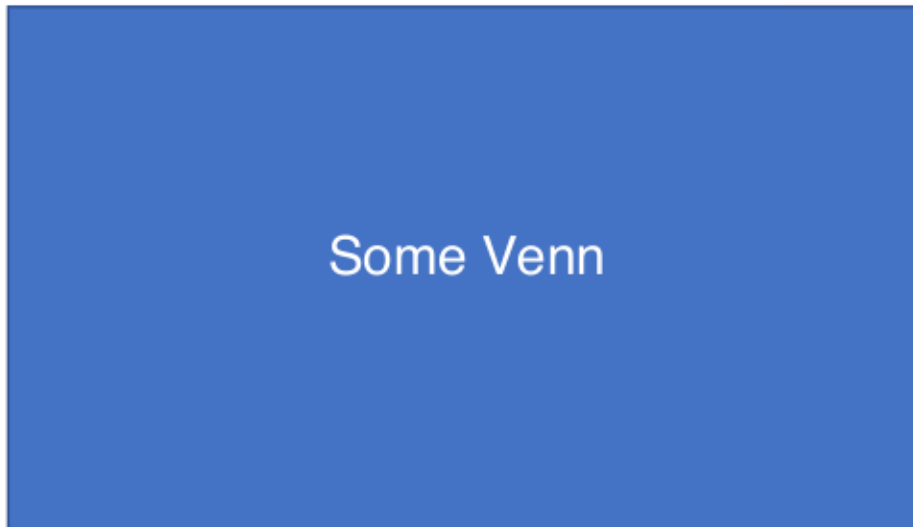
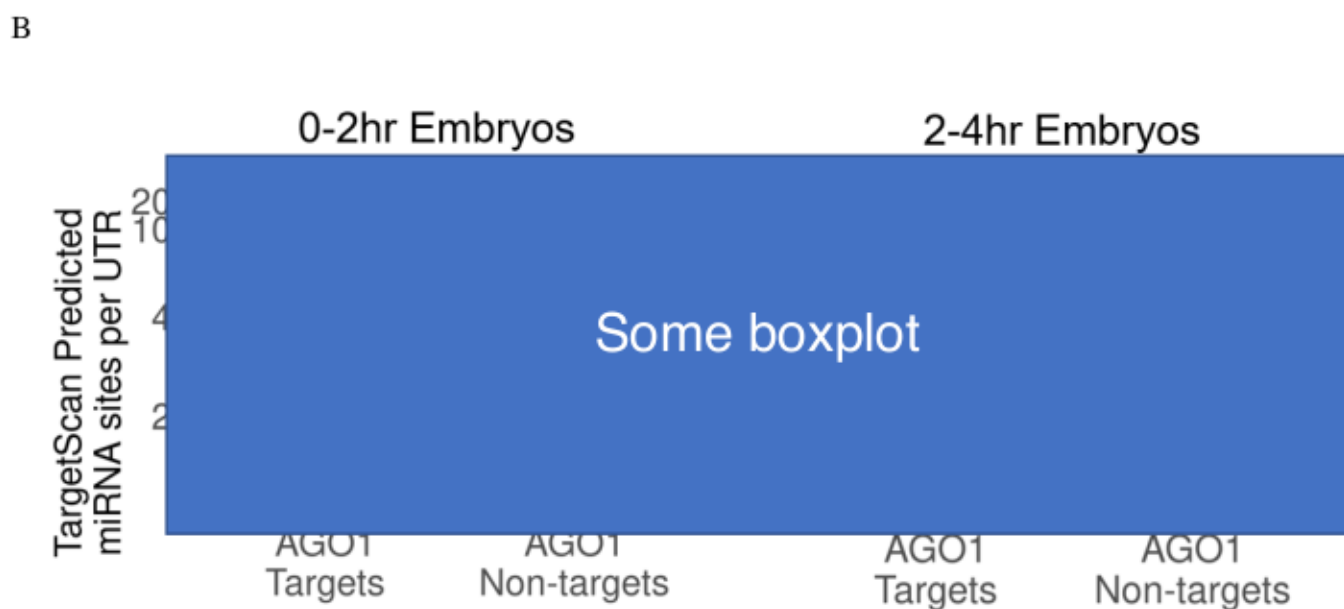
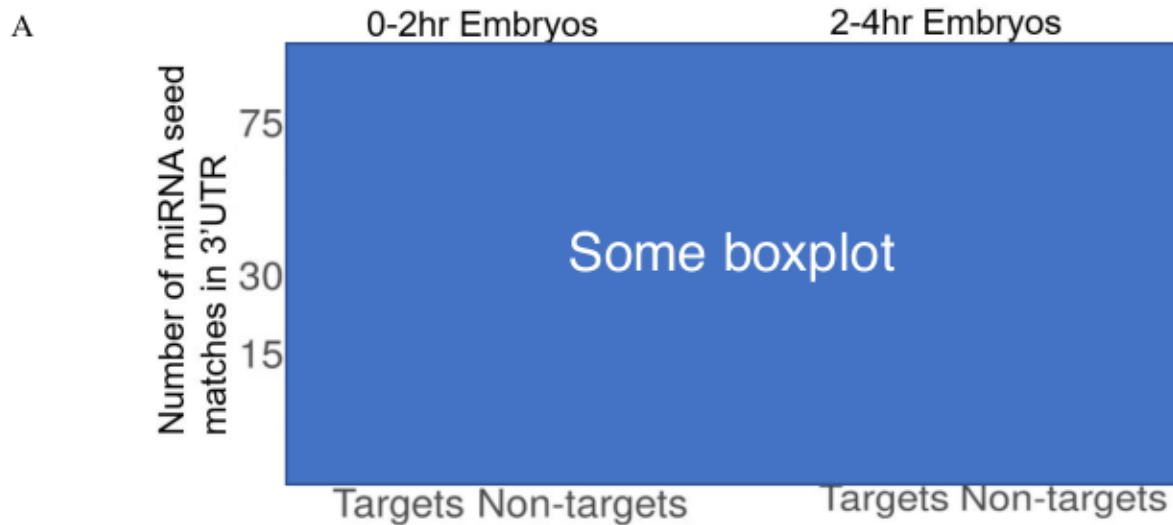


Figure 1: Identify miRISC targets in early embryos by RIP-seq.

Total RNA extracted from 0-2hr or 2-4hr old embryos were subject to anti-AGO1 IP or control IP with an irrelevant IgG, and three replicates for each condition were sequenced together with total input as background. (A) is a schematic of the data processing pipeline. Raw reads from RNA-seq were trimmed, filtered, and mapped before enrichment analyses for target identification by DESeq2. (B) Expressed genes (TPM > 1 in all three input replicates) are kept for analysis, and enrichment is defined as a minimal of 1.5-fold enrichment (\log_2 fold change > 0.58, represented by dashed lines) over total input with $P < 0.05$. miRISC targets are genes enriched in AGO1 IP but not in control IP, represented by orange dots. xxxx genes are identified as targets out of xxxx in 0-2hr embryos, and xxxx are identified out of xxxx in 2-4hr embryos. (C) Using a total of xxxx genes detected in 0-4hr embryos as background, targets identified from the two points overlap significantly.



D



E

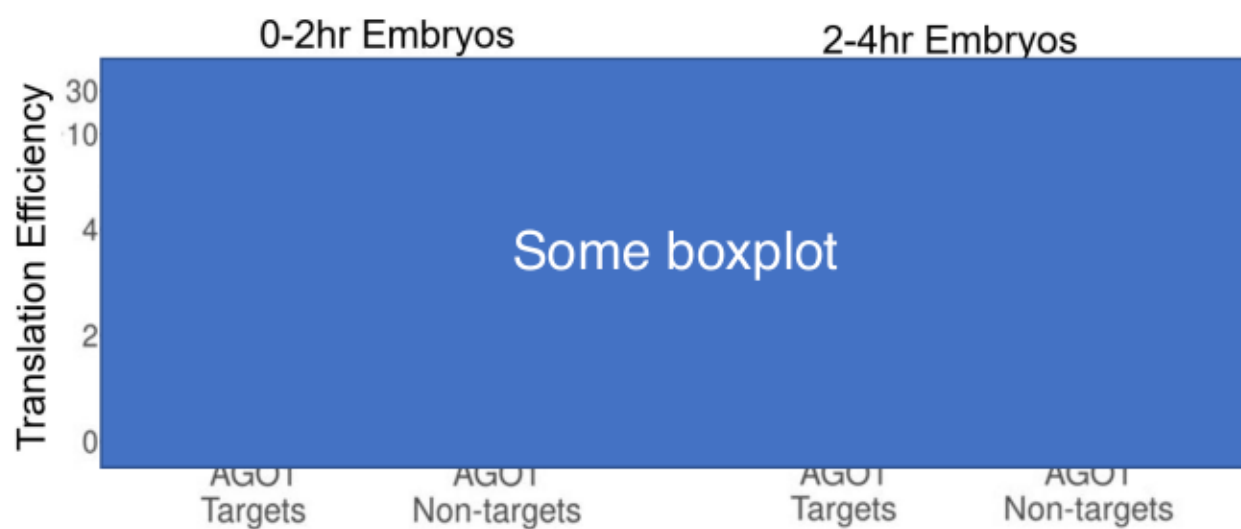


Figure 2: AGO1 targets are enriched for miRNA seed matches, unstable transcripts, and translationally repressed transcripts.

Seed region refers to nucleotides 2-7 of a miRNA, and xxxx different seeds are expressed in 0-4hr embryos. The most abundant isoform of expressed genes was used for A-D, while E was analyzed at the gene level. (A) Total number of predicted matches to expressed seeds were counted for each transcript's 3' UTR, and AGO1 targets contain significantly more matches than non-targets in both time points. (B) TargetScan database was used to predict miRNA-mRNA binding, and a similar result is observed. (C) Accessibility of each miRNA match site on one 3'UTR is assessed based on RNA secondary structure and is represented by a score between 0 and 1 (1 suggests the site is always available for miRNA binding). The average score of the most available site for each miRNA is calculated, and AGO1 targets harbor more accessible sites for miRNA on their 3'UTRs. (D) Transcriptome of early embryo is grouped into xxxx clusters based on their expression profiles. AGO1 targets are enriched for 4 clusters (highlighted in red boxes), where all of them contain a degradation component. For both time points, about 40% of the hits belong to cluster 7/8. These hits cover about xxxx% and xxxx% of cluster 7/8 genes at 0-2hr and 2-4hr time point, respectively. (E) information on translation efficiency is extracted from an external dataset¹⁹. AGO1 targets have lower translation efficiency compared to non-targets in both time points.

A

| Odds Ratio | GO Term |
|------------|---------|
| | Term 1 |
| | Term 2 |
| | |
| | |
| | |
| | |

B

[illegible]

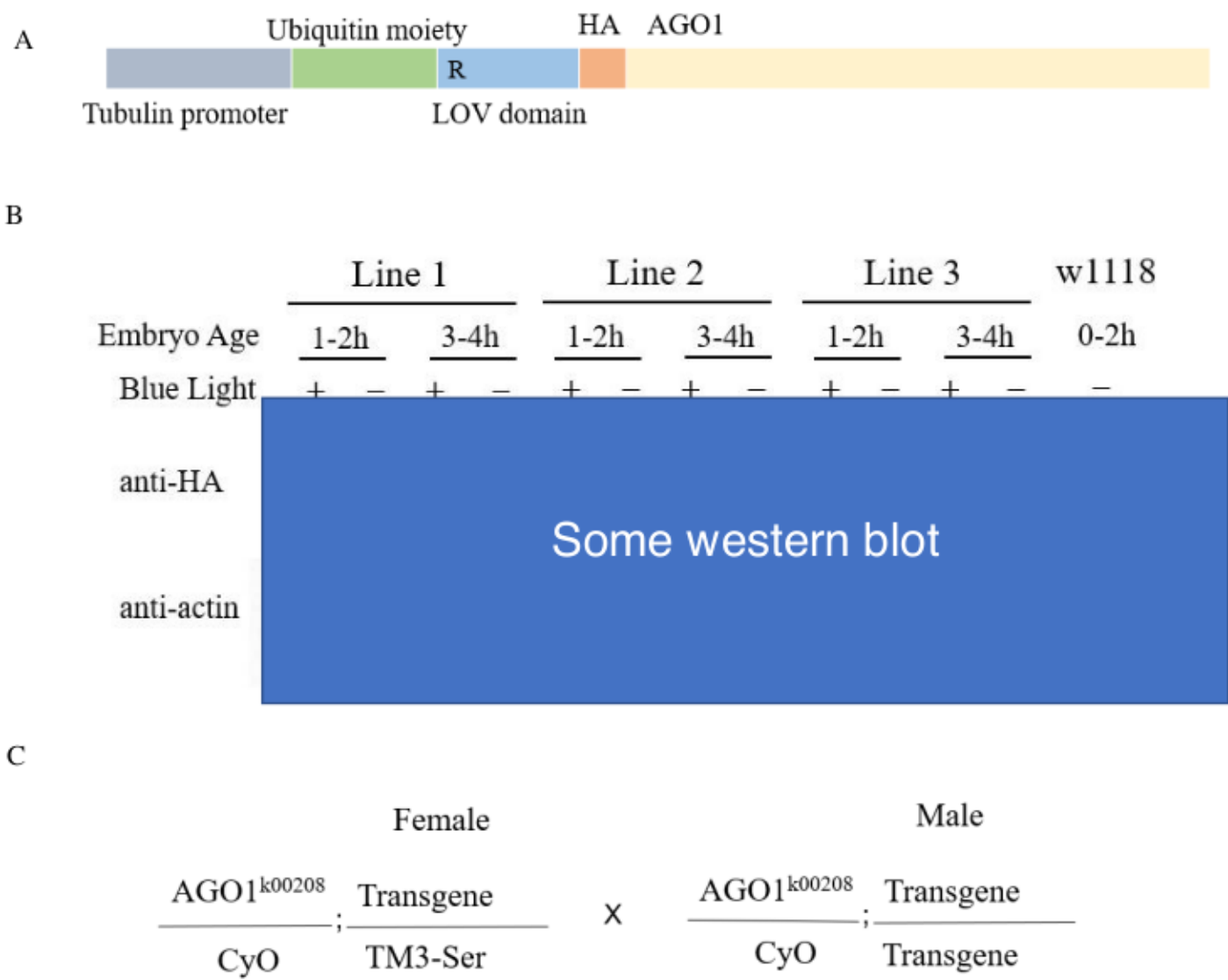
C

| Odds Ratio | GO Term |
|------------|---------|
| | Term 1 |
| | Term 2 |
| | |
| | |
| | |

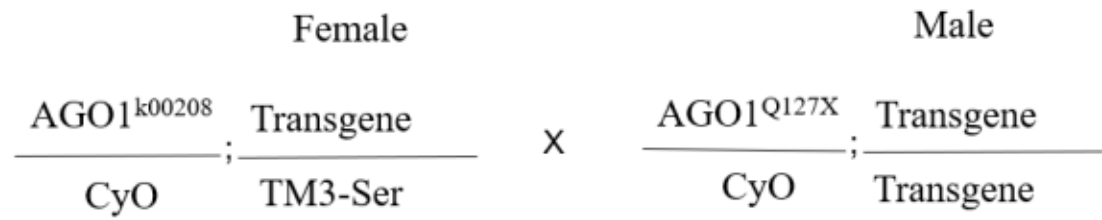
D

| Transcription Factor | Gene Function |
|----------------------|---------------|
| Gene 1 | |
| Gene 2 | |
| | |
| | |
| | |

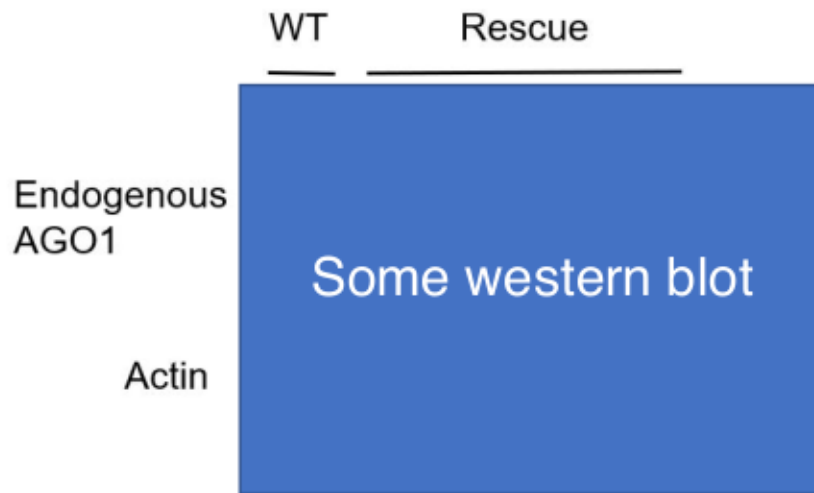
Figure 3: miRISC regulate ____ processes.
 GO Term enrichment analysis was performed for AGO1 targets. (A) xxxx ____ terms with largest odds ratio are listed, these terms cover various aspects under the umbrella of cytoskeleton. (B) 20 most enriched genes in AGO1 RIP-Seq are listed for each time point. About half of the genes from each list are ____term-relevant (highlighted in blue). (C) 5 ____ with largest odds ratio are listed. ____ signaling participates in ____ regulation, while other signaling events involve in fundamental processes in early embryo such as _____. (D) 5 enriched genes are listed. Some are downstream of signaling pathways in (C). gene x is an interesting target because it is required for ZGA, an early developmental event happens during the MZT.



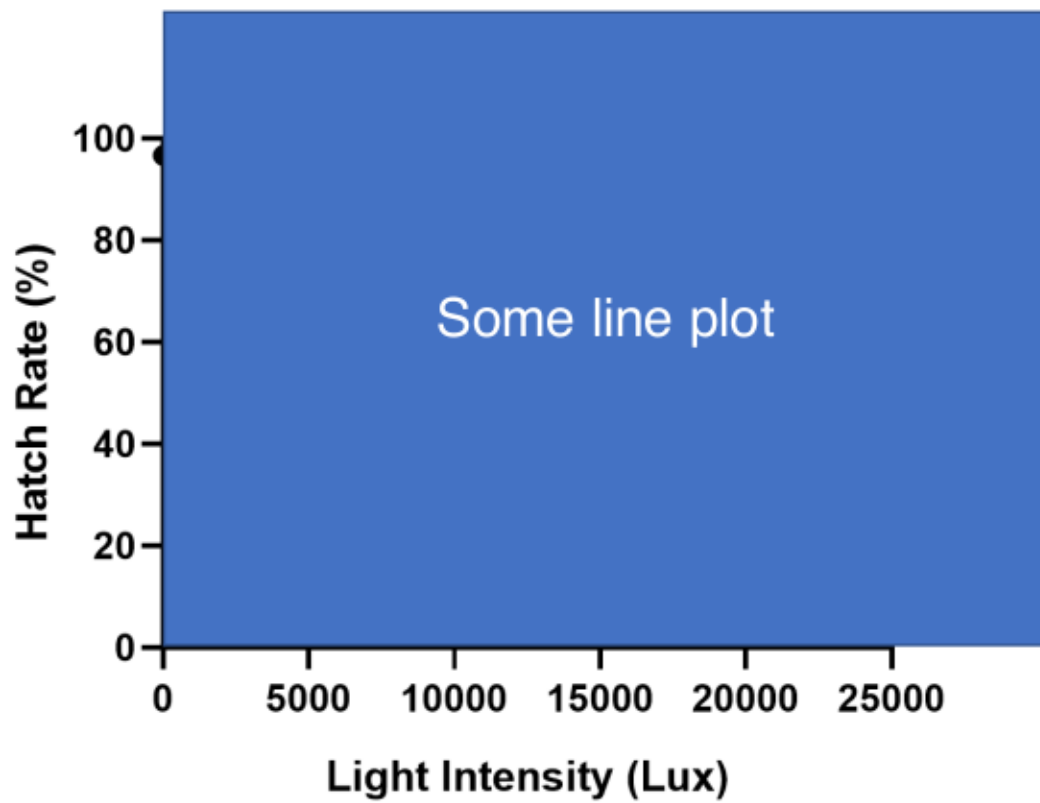
D



E



F



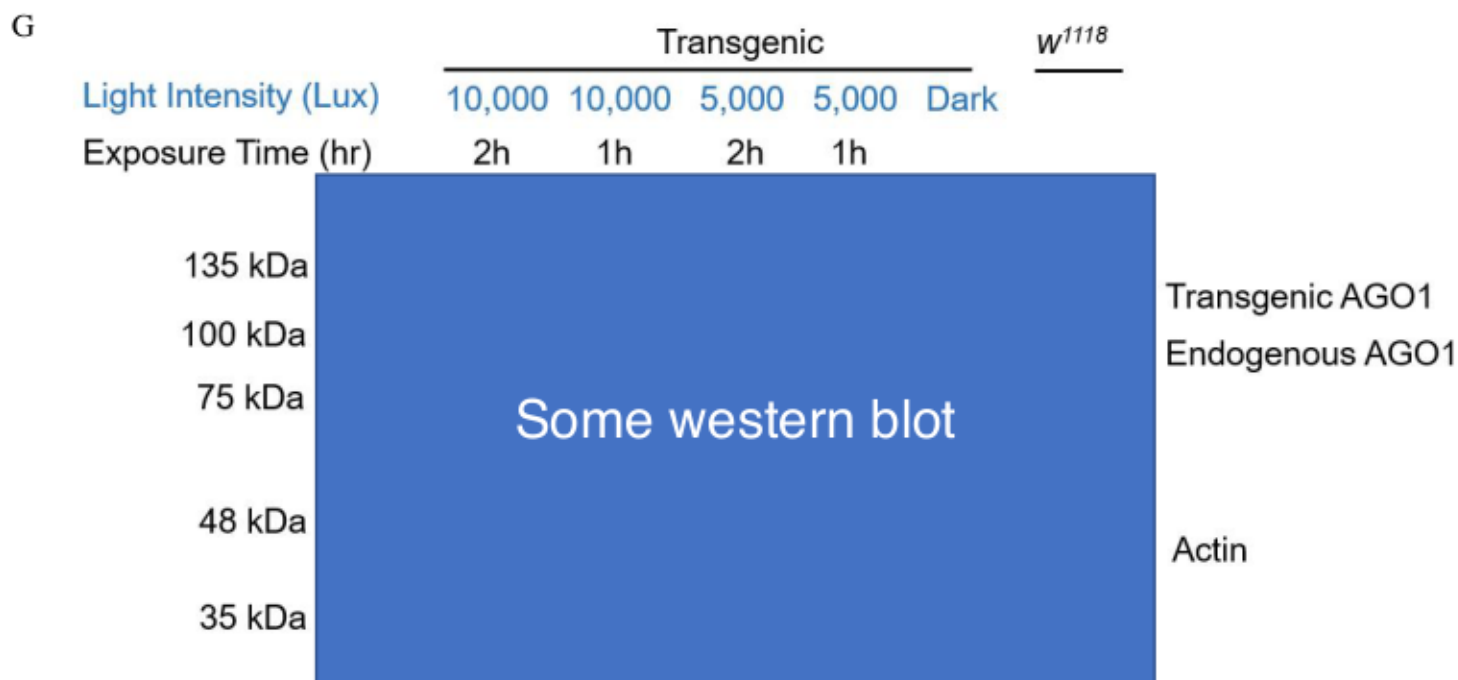


Figure 4: the transgene is degraded upon blue light exposure and rescues loss of AGO1.

(A) Design of the AGO1 transgene. Response to blue light is rendered by the LOV domain depicted in blue, which unfolds upon blue light irradiation, exposes an N terminal arginine and leads to protein degradation. A ubiquitin moiety (in green) is fused to the N terminus of the LOV domain to generate the N-terminal Arg residue. An HA epitope enables convenient detection of the protein. This construct is driven by a tubulin promoter to achieve high level of expression.

(B) Three lines with AGO1 transgene were tested to confirm blue-light-inducible protein degradation. All three lines show higher protein level at 3-4hr than at 1-2hr, which is consistent with the steady AGO1 upregulation in early embryos. 3-4hr samples with blue light exposure showed an obvious decrease in AGO1 protein level compared to samples of the same age but without light exposure. (C, D) two crossing schemes with the attempt to obtain rescue flies. (E) rescue flies obtained following scheme (C), and Western blot was performed using female ovary to confirm loss of endogenous AGO1 expression. (F) Hatch rate is the percentage of embryos that complete embryogenesis successfully. 4h of blue light exposure with indicated light intensity is not phototoxic to 0-1hr *w¹¹¹⁸* embryos. (N=3) (G) Different exposure time and light intensity was tested using a line that rescues in (C, E). Longer exposure time is better for both light intensity groups, but counterintuitively, the lower intensity achieves better clearance.

A

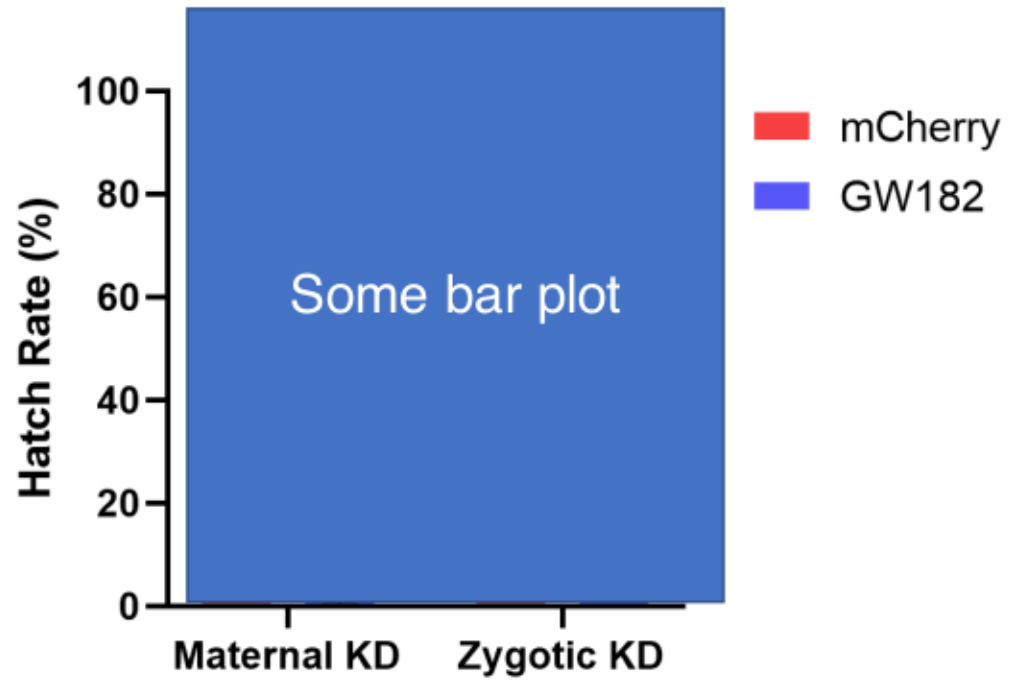


Figure 5: GW182 is required maternally.

Hatch rate is the percentage of embryos that complete embryogenesis successfully. (A) Maternal or zygotic knockdown (KD) of GW182 was performed using RNAi, and only maternal KD leads to a large drop in hatch rate (N=3).

References

1. Vastenhouw, N. L., Cao, W. X., & Lipshitz, H. D. (2019). The maternal-to-zygotic transition revisited. *Development*, 146(11). <https://doi.org/10.1242/dev.161471>
2. Lécuyer, E., Yoshida, H., Parthasarathy, N., Alm, C., Babak, T., Cerovina, T., Hughes, T. R., Tomancak, P., & Krause, H. M. (2007). Global Analysis of mRNA Localization Reveals a Prominent Role in Organizing Cellular Architecture and Function. *Cell*, 131(1), 174–187. <https://doi.org/10.1016/j.cell.2007.08.003>
3. Thomsen, S., Anders, S., Janga, S. C., Huber, W., & Alonso, C. R. (2010). Genome-wide analysis of mRNA decay patterns during early *Drosophila* development. *Genome Biology*, 11(9), R93. <https://doi.org/10.1186/gb-2010-11-9-r93>
4. Tadros, W., Goldman, A. L., Babak, T., Menzies, F., Vardy, L., Orr-Weaver, T., Hughes, T. R., Westwood, J. T., Smibert, C. A., & Lipshitz, H. D. (2007). SMAUG Is a Major Regulator of Maternal mRNA Destabilization in *Drosophila* and Its Translation Is Activated by the PAN GU Kinase. *Developmental Cell*, 12(1), 143–155. <https://doi.org/10.1016/j.devcel.2006.10.005>
5. Laver, J. D., Li, X., Ray, D., Cook, K. B., Hahn, N. A., Nabeel-Shah, S., Kekis, M., Luo, H., Marsolais, A. J., Fung, K. Y., Hughes, T. R., Westwood, J. T., Sidhu, S. S., Morris, Q., Lipshitz, H. D., & Smibert, C. A. (2015). Brain tumor is a sequence-specific RNA-binding protein that directs maternal mRNA clearance during the *Drosophila* maternal-to-zygotic transition. *Genome Biology*, 16(1). <https://doi.org/10.1186/s13059-015-0659-4>
6. Iwakawa, H. O., & Tomari, Y. (2022). Life of RISC: Formation, action, and degradation of RNA-induced silencing complex. *Molecular Cell*, 82(1), 30–43. <https://doi.org/10.1016/j.molcel.2021.11.026>
7. Neumüller, R. A., Betschinger, J., Fischer, A., Bushati, N., Poernbacher, I., Mechtler, K., Cohen, S. M., & Knoblich, J. A. (2008). Mei-P26 regulates microRNAs and cell growth in the *Drosophila* ovarian stem cell lineage. *Nature*, 454(7201), 241–245. <https://doi.org/10.1038/nature07014>
8. Schwamborn, J. C., Berezikov, E., & Knoblich, J. A. (2009). The TRIM-NHL Protein TRIM32 Activates MicroRNAs and Prevents Self-Renewal in Mouse Neural Progenitors. *Cell*, 136(5), 913–925. <https://doi.org/10.1016/j.cell.2008.12.024>
9. Luo, H., Li, X., Claycomb, J. M., & Lipshitz, H. D. (2016). The Smaug RNA-Binding Protein Is Essential for microRNA Synthesis During the *Drosophila* Maternal-to-Zygotic Transition. *G3 Genes|Genomes|Genetics*, 6(11), 3541–3551. <https://doi.org/10.1534/g3.116.034199>
10. Bushati, N., Stark, A., Brennecke, J., & Cohen, S. M. (2008). Temporal Reciprocity of miRNAs and Their Targets during the Maternal-to-Zygotic Transition in *Drosophila*. *Current Biology*, 18(7), 501–506. <https://doi.org/10.1016/j.cub.2008.02.081>
11. Krueger, F. (2021). FelixKrueger/TrimGalore: v0.6.7. <https://zenodo.org/record/5127899>
12. Kopylova, E., Noé, L., & Touzet, H. (2012). SortMeRNA: fast and accurate filtering of ribosomal RNAs in metatranscriptomic data. *Bioinformatics*, 28(24), 3211–3217. <https://doi.org/10.1093/bioinformatics/bts611>
13. Patro, R., Duggal, G., Love, M. I., Irizarry, R. A., & Kingsford, C. (2017). Salmon provides fast and bias-aware quantification of transcript expression. *Nature Methods*, 14(4), 417–419. <https://doi.org/10.1038/nmeth.4197>

14. Love, M. I., Huber, W., & Anders, S. (2014). Moderated estimation of fold change and dispersion for RNA-seq data with DESeq2. *Genome Biology*, 15(12).
<https://doi.org/10.1186/s13059-014-0550-8>
15. McGeary, S. E., Lin, K. J., Shi, C. Y., Pham, T., Bisaria, N., Kelley, G. M., & Bartel, D. P. (2019). The biochemical basis of microRNA targeting efficacy. *Science*, 366(6472).
<https://doi.org/10.1126/science.aav1741>
16. Li, X., Quon, G., Lipshitz, H. D., & Morris, Q. (2010). Predicting in vivo binding sites of RNA-binding proteins using mRNA secondary structure. *RNA*, 16(6), 1096–1107.
<https://doi.org/10.1261/ma.2017210>
17. Kolberg, L., Raudvere, U., Kuzmin, I., Vilo, J., & Peterson, H. (2020). gprofiler2 -- an R package for gene list functional enrichment analysis and namespace conversion toolset g:Profiler. *F1000Research*, 9, 709. <https://doi.org/10.12688/f1000research.24956.1>
18. Eichhorn, S. W., Subtelny, A. O., Kronja, I., Kwasniewski, J. C., Orr-Weaver, T. L., & Bartel, D. P. (2016). mRNA poly(A)-tail changes specified by deadenylation broadly reshape translation in *Drosophila* oocytes and early embryos. *ELife*, 5.
<https://doi.org/10.7554/elife.16955>
19. Stevens, L. M., Kim, G., Koromila, T., Steele, J. W., McGehee, J., Stathopoulos, A., & Stein, D. S. (2021). Light-dependent N-end rule-mediated disruption of protein function in *Saccharomyces cerevisiae* and *Drosophila melanogaster*. *PLOS Genetics*, 17(5), e1009544.
<https://doi.org/10.1371/journal.pgen.1009544>

Proposal Outline

I propose a transcriptome-wide investigation of miRISCs function during the fly MZT and have two specific aims. They are:

1. Identify miRISC targets during the MZT.
2. Elucidate the mechanism of miRISC during the MZT.

Aim 1: Identify miRISC targets during the MZT.

Aim 1.1: Identify miRISC-bound transcripts biochemically by RIP-Seq. IP and sequencing were done before I joined the lab, and I started with analyzing the sequencing results. By now, I have computationally identified and validated AGO1 targets, thus this aim is largely complete. I have also identified several biological processes that miRISC targets may regulate, including cytoskeletal dynamics, signaling pathways, body segmentation and tissue differentiation. The follow-up experiments will be discussed in Aim 1.3.

Aim 1.2: Identify miRISC-regulated transcripts genetically. Because AGO1^{-/-} is lethal, the goal of aim 1.2 is to achieve temporary deletion of AGO1 protein in early embryos. The current design is to express a fusion protein of AGO1 and a light-inducible degron. I have confirmed that the transgenic protein responds to blue light and can rescue lethality and female fecundity. My first attempt is to develop a rescue fly stock and obtain loss-of-AGO1 embryos. If the first attempt failed, the next approach is to mate rescue females to wild-type males because the zygotic contribution of endogenous AGO1 level may be negligible during the time frame of interest (0-4hr). If it turns out to be true, I will collect these embryos as a loss-of-AGO1 model. In the worst case, I will apply the conventional RNAi approach to knockdown AGO1.

Aim 1.3: Assess miRISC's role in loss-of-AGO1 embryos.

I will first examine the level of several confident AGO1 targets from Aim 1.1 by RT-qPCR and Western blot, when suitable antibodies are available. Because miRISC induces transcript decay/translational repression, I would expect mRNA and protein upregulation. Then to determine whether miRISC regulates identified signaling pathways and transcription factors, I will search the literature for genes whose transcription is regulated by these pathways/factors and ask if they are misregulated when AGO1 function is disrupted. If results from single targets are promising, I will then collect loss-of-AGO1 embryos for RNA-seq, analyze the dataset similar to Aim 1.1, and ask if the target genes of the pathways/factors behave as expected. To evaluate miRISC's role in cytoskeletal dynamics, I will perform fluorescence staining in early embryos. DAPI staining may reveal general defects in the nuclear division, phalloidin will enable actin filament visualization, and anti-peanut staining reflects cytokinesis and thus microtubule function.

Aim 2: Elucidate the mechanism of miRISC during the MZT.

In the current model for miRISC function, miRISC recruits deadenylase CCR4/NOT through GW182 to trigger transcript decay. However, this miRISC-deadenylase interaction is not detected in early embryos. To determine whether GW182 and CCR4/NOT are required for miRISC function, I will knockdown both genes maternally and zygotically and examine mRNA/protein levels of miRISC targets (as in Aim 1.3). If GW182 is required, I will then screen GW182 interactors identified through IP-MS and evaluate their importance in miRISC function. Otherwise, I will perform IP-MS against AGO1 in early embryos and then screen AGO1 interactors as described above for GW182. If CCR4/NOT is required, I will confirm miRISC targets are deadenylated and further explore the recruiting mechanism of it. Literature has also suggested that miRISC may induce silencing mainly through translational repression, and I will investigate this possibility with a GFP reporter.